

Final Project Report

High-resolution P- and S-Wave Velocity Structure of the Post-Paleozoic Sediments in the Upper Mississippi Embayment: Collaborative Research between the University of Kentucky and the University of Memphis

Jer-Ming Chiu
Center for Earthquake Research and Information
The University of Memphis
Memphis, TN 38152
jerchiu@memphis.edu

Edward Woolery
Department of Geological Sciences
University of Kentucky
Lexington, Kentucky
ewoolery@uky.edu

USGS Project: 06HQGR0049 (UoM) and 06HQGR0145(UK)

Project Duration: March 1, 2006 – September 30, 2007

Abstract

Site response, sedimentary basin geometry, earthquake induced strong ground motion, distribution of earthquake hypocenters, and geometry and characteristic feature of active faults are among the most essential elements for seismic hazard assessment in the upper Mississippi Embayment. However, these elements cannot be successfully evaluated without reliable Vp and Vs information for the embayment sediments. Under the current USGS NEHRP project support, 20 sites in the northern Mississippi Embayment were selected for field experiment to explore detail Vp and Vs structural information. At each selected site, a seismic reflection/refraction line has been conducted using a seismic source that generates both P- and S-waves. For sites not near any regional seismic network stations, a temporary portable broadband seismic station has been installed for a few weeks to record local earthquakes. Seismic data from the reflection/refraction line and from the recorded local earthquakes are analyzed to explore the Vp and Vs structures of the post Paleozoic sediments beneath each site. The Vp and Vs structures for the sediments beneath adjacent sites are then compared to explore lateral velocity structural variations. Preliminary results reveal that seismic velocities and lithologic features of the sediments in the embayment are characterized by extremely low seismic velocity, especially Vs, near surface and by very significant lateral and vertical variations. The sediments in the Upper Mississippi Embayment cannot be described simply by any 1-D homogeneous horizontally layered velocity model, typically obtained from surface wave analysis and from long seismic refraction profiles. Thus, earthquake locations as well as seismic hazard assessment cannot be properly determined without more detail 3-D Vp and Vs structural models for the sediments in the Upper Mississippi Embayment.

Introduction

The New Madrid seismic zone (NMSZ) (Figure 1) is currently the most seismically active region in the United States east of the Rocky Mountains (Johnston, 1982). Potential for future damaging earthquakes along the NMSZ is the highest in the central and eastern U.S. The active seismic zone lies beneath the thick deposit of sediments in the upper Mississippi Embayment. Site response, sedimentary basin geometry, earthquake induced strong ground motion, distribution of

earthquake hypocenters, and geometry and characteristic feature of active faults are among the most essential elements for seismic hazard assessment in the upper Mississippi Embayment. However, these elements cannot be successfully evaluated without reliable Vp and Vs information for the embayment sediments.

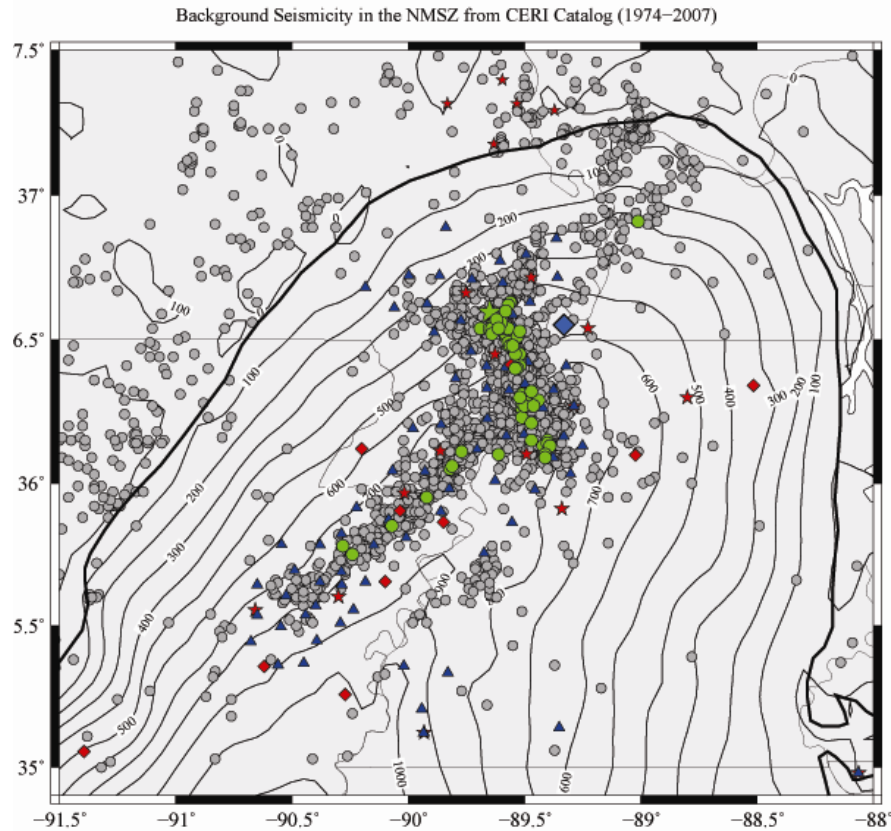


Figure 1. Background seismicity (gray circles) in the New Madrid seismic zone of the central U.S. along with the boundary of the Mississippi Embayment (thick line) and contour lines of the bottom of the sediments (thin lines). Solid green circles are recent earthquake locations during the period of broadband deployment. Red diamonds are the locations of deep wells with logs that reach to the bottom of the sediments. Blue triangles and red stars are the short-period and broadband CERI network stations, respectively. Blue diamond is the location of UK's deep drilling site where the Paleozoic basement is reached at 585 m. The study area is north of 35° N inside the boundary of the embayment.

Local soil conditions can have a profound influence on the characteristics of ground shaking during a large earthquake as observed from many modern damaging earthquakes, e.g. the 1985 Mexico, the 1988 Armenia, the 1989 Loma Prieta, the 1994 Northridge, the 1999 Chi-Chi, Taiwan, and the 2001 Gujarat, India. These examples highlight the importance of how local soil conditions affect ground motions responsible for damages and casualties. As a first order approximation, site specific soil classifications and Vs30 information have been adapted by the NEHRP standard to estimate site amplification and to predict strong ground motion, e.g. Cramer (2001, 2006), Gomberg et al. (2003), and Cramer et al. (2004) for seismic hazard maps in the Memphis and embayment area, Williams et al. (1997) for Seattle, Washington, and Wills et al. (1998) for large scale seismic hazard maps in California. In most cases, the contribution of large impedance contrast in the shallow sediments is not properly introduced in seismic hazard assessment, most probably due to lack of detail site-specific velocity information for the sediments.

Over the last decade, direct (e.g. shallow boreholes) and indirect (e.g. seismic lines and earthquakes) methods have been applied at many sites in the Upper Mississippi Embayment to

measure V_s in shallow sediments, to determine soil profiles as a function of depth, and to study attenuation of seismic waves in the unconsolidated sediments. From these efforts, the V_s averaged to 30 m depth (V_{s30}) has commonly been referred as an indicator to predict earthquake ground-motion amplification, and to form the basis of site hazard classification under National Earthquake Hazard Reduction Program-Uniform Building Code (NEHRP-UBC). Site specific amplification maps have been constructed for a few basins in the US based on the soil classification and V_{s30} information. However, results of a few previous shallow seismic profiles in the central New Madrid Seismic Zone (NMSZ) reveal that the largest amplification may corresponding to the largest impedance (velocity and density) contrast at a depth around 100 m inside the sedimentary basin. Examples of deep borehole vertical seismic array observations in other basins reveal that a large velocity contrast at a depth ~ 60 m is responsible for a significant amplification to double its peak ground acceleration (PGA) from the bottom of a basin. Therefore, high-resolution V_p and V_s profiles for the entire sediments are essential to quantify the site specific amplification factor that may not be properly represented simply by the general information of V_{s30} and soil classifications. This is particular true for the Mississippi Embayment.

In this collaborative USGS project, V_p and V_s information for the entire sediment column beneath 20 selected sites are explored by combining short seismic reflection/refraction lines, well logs, and on-site recording of local earthquake waveforms. Our preliminary results confirm that seismic velocities and lithologic features of the sediments in the embayment are characterized by very significant lateral and vertical variations and that they cannot be described simply by any 1-D homogeneous horizontally layered velocity model, typically obtained from surface wave analysis and from long seismic refraction profiles.

The sedimentary basin in the upper Mississippi Embayment is a south-plunging synclinal trough, characterized by gently south dipping post-Paleozoic sediments that thicken southward and toward the central axial line of the embayment. The southern end of the seismic zone, near Memphis Tennessee, has a sediment thickness of nearly 1000 m. Within the sedimentary basin, significant lateral and vertical variations of sediment's properties are commonly observed from a few deep well-logs (Dart, 1992; Gao 1999). Results from a few shallow seismic lines conducted in the mid to late 90s by the University of Kentucky (UK) near the New Madrid area (e.g. Street et al., 1995) reveals further that the interface at ~ 100 m (Figure 2) may contribute to the most significant amplification beneath these sites due to large impedance contrast. Depth and impedance contrast of these interfaces vary slightly even though these sites are relatively close. Preliminary results from the 20 deep seismic profiles conducted during our recent collaborative USGS project demonstrate further that the site specific amplification factor as well as the predicted strong ground motion cannot be estimated simply from V_{s30} and soil classification information alone. Therefore, characteristic features of the complicated sedimentary basin in the embayment cannot be adequately described by a simple 1-D homogeneous horizontally layered model (e.g. Chiu et al., 1992; Dorman and Smalley 1994). Future improvement for seismic hazard assessment in the upper Mississippi Embayment will have to rely on better determined 3-D V_p and V_s models for the entire sedimentary basin.

In addition, earthquake-induced ground motions in the upper Mississippi Embayment are expected to be predominantly a function of Q_s in the deeper velocity structure, and a function of shear-wave velocities and vertical variations of properties of the near-surface soils (Street et al. 2001; Williams et al. 2001). However, unexpected ground motions from a moderate to large earthquake ($M_w \geq 6$) could be produced from P/ S_v wave coupling of non-vertically incident waves, trapped body waves, locally generated surface waves arising from the conversion of S-waves to

surface waves at the boundary of the sediment-filled basin (Frankel et al. 2001), spatial variations caused by irregular geometry in the bedrock-sediment interface, and/or horizontal variations in the seismic velocity and density, focusing effect by the geometry of the basin, etc. Possible effects might also include broadband amplification, resonance at frequencies other than those predicted by 1-D modeling, and substantially longer durations in ground motions (particularly at the longer periods), such as those observed by Carver and Hartzell (1996) in the Santa Cruz Basin from aftershocks of the 1989 Loma Prieta, California, earthquake.

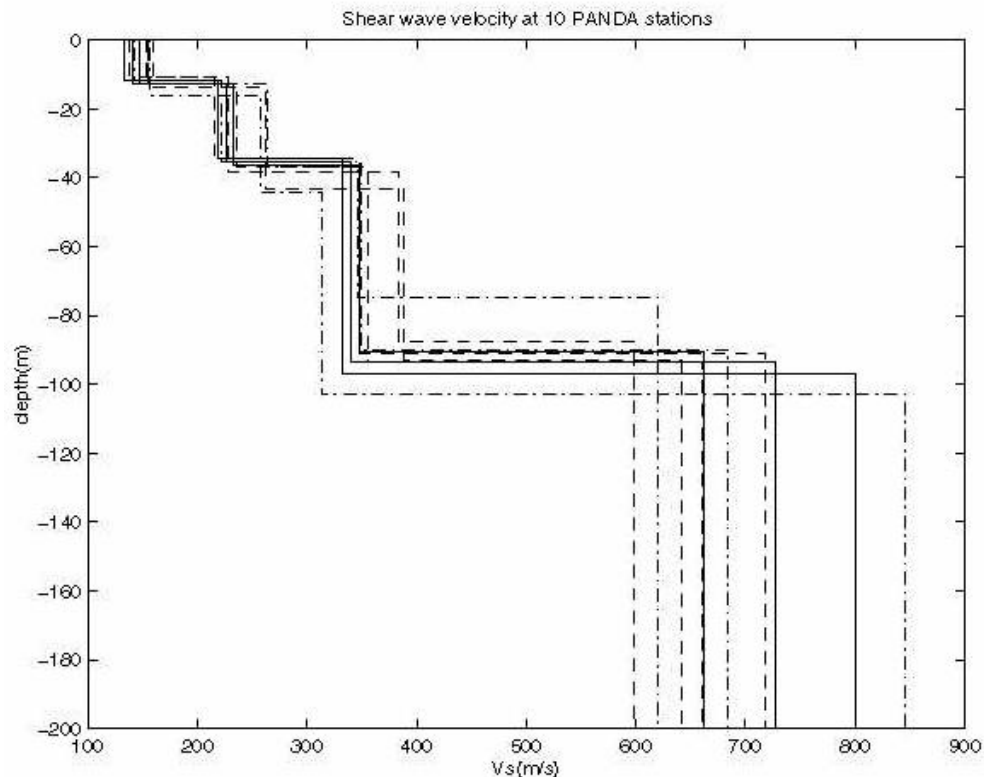


Figure 2. Shallow Vs profiles from seismic reflection/refraction lines near 10 PANDA stations showing that Vs is slower than the speed of sound in air in the upper most 100 meters of sediments. Very significant variations on depths of interfaces and interval Vs are apparent even when these sites are adjacent to each other. The large impedance contrast across the sedimentary layer boundary at a depth ~100 m will most probably contribute to the most significant site-specific amplification for the incoming seismic waves.

It is also well recognized that geometry of the sedimentary basin and seismic velocity distribution inside a basin are the two essential elements to our investigation of how the sedimentary basin responds to the incoming strong seismic waves. Better determined velocity information inside the sedimentary basin will also improve significantly on the reliability of earthquake hypocenters, especially their depth distributions; from which active fault geometry and its characteristic features will be better understood. All these issues are important for a successful NEHRP program and the keys to address these issues rely primarily on the determination of reliable Vp and Vs models for the sediments in the entire upper Mississippi Embayment.

Previous Studies of Velocity Models for the Sedimentary Basin

As a first order approximation, most currently available Vp and Vs models for the embayment sediments (e.g. Chiu et al., 1992; Dorman and Smalley, 1994; Gao, 1999) are characterized by over-simplified thin homogeneous sedimentary layers. This is due to very few direct velocity measurements in a large area and the fact that properties of the loosely

unconsolidated soil, especially at the upper most 100 meters, vary significantly as a function of depth and location. Although there are at least 45 deep wells (10 with lithologic and sonic logs) to the bottom of the sediments (e.g. Dart 1992; Gao 1999), they are sparsely distributed over a large area in the upper Mississippi Embayment (Figure 1). Not only there is lack of V_s information from these deep wells but also logs for the upper most 100 m (in some cases ~200 m) are usually not available. A few in-situ downhole measurements have provided direct V_p and V_s information for the very shallow sediments (e.g. Liu et al., 1997). However, only very few measurements have been done outside of the Shelby County which constitutes only a small portion of the upper Mississippi Embayment. Recently, V_s information for the embayment was included in the CUSEC database (Bauer, 2004) but this data is also limited at very shallow depths. Therefore, a meaningful assessment of seismic response of the sediments for the entire upper Mississippi Embayment is hindered by the lack of broader, deeper, systematic, and reliable velocity measurements, especially the V_s , for the entire sedimentary basin.

It is well-recognized that the large impedance contrast across the bottom of the sediments will contribute to the first major amplification of the incoming strong motion. The impedance contrast, especially for the V_s , is also expected to be very high across the boundary between the compacted and the loosely unconsolidated sediments at a shallow depth, which is expected to be different between sites due to different depositional history. Whether the site-specific amplification occurs at depth ~100 m as shown in the central NMSZ region (Figure 2) or at a depth ~60 meters similar to the examples shown in a set of borehole array data in the Taipei basin (Figure 3) or at different depths is an important topic that needs to be addressed in order to successfully estimate seismic response and strong ground motion expected in the region.

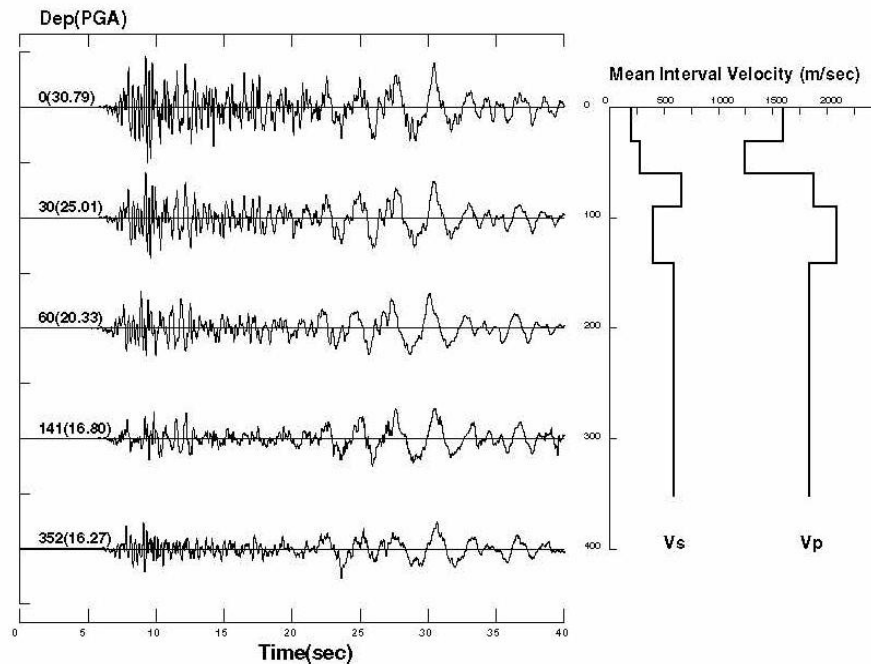


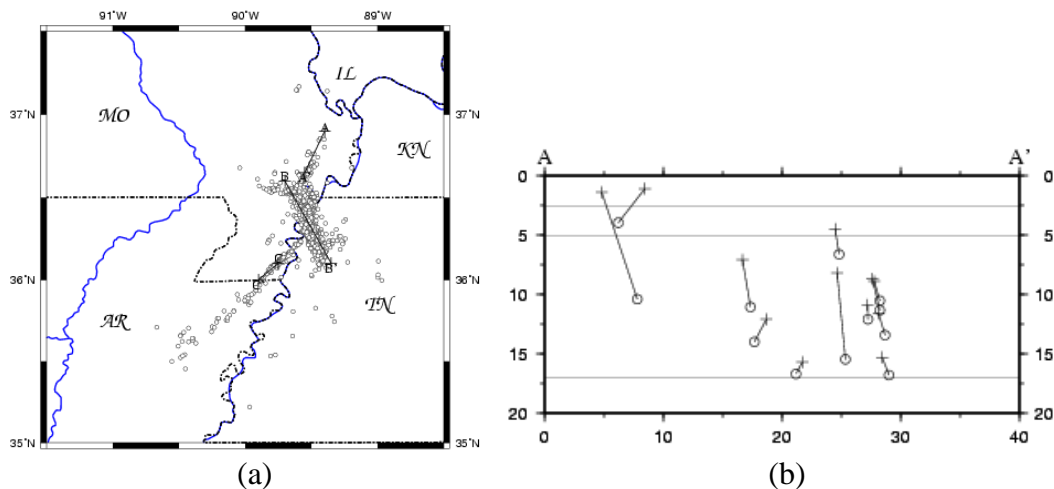
Figure 3. Examples of strong motion seismograms (left) from a borehole array in western Taipei basin (Chen, 2003) and V_p and V_s profiles determined from well-logs (right) (Wen et al., 1995). Depths of the borehole instruments range from 352 meters to surface with peak ground accelerations (PGA) range from 16.27 to 30.79 cm/sec^2 , respectively. It is clear that the amplitude of the incoming strong motion as indicated by the PGA is amplified significantly across the boundaries of very significant impedance contrast, especially in the shallow depth at 60 meters for the S waves where the PGA value is doubled from the bottom.

In the mid 1980s, a layer of 0.65 km thickness with $V_p=1.8$ km/sec was suggested to represent the sediments in the upper Mississippi Embayment from the interpretation of a few long

seismic refraction lines (e.g. Mooney et al., 1983; Andrews et al., 1985). The V_s of the sedimentary layer was introduced under an assumption of $V_p/V_s = 3.21$ from similar sediments elsewhere. From a 1-D velocity inversion of 3-component PANDA data in the central NMSZ region, Yang (1992) and Chiu et al. (1992) provided the first estimation of average V_s of 0.6 km/sec for the sedimentary layer which leads to a $V_p/V_s = 3.0$.

From their study of converted waves generated from the bottom of the sediments, Chen et al. (1994, 1996) concluded that incident P- and S-waves from any NMSZ earthquake will propagate almost vertically to the surface, also generating efficiently large amplitude converted waves across the interface between the overriding sediments and the underlying Paleozoic basement. Chen et al. (1996) were able to estimate the variations of average V_s of the sediments in the ranges from 0.45 to 0.67 km/sec beneath the 40 PANDA stations in the central NMSZ. They concluded that the regions of higher average V_s could be correlated to the denser and more compact sediments in the lower part of the thick sediments. Pujol et al. (1997) pointed out that V_p and V_s of the sedimentary section is not a constant from a JHD analysis of earthquake data. Liu et al. (1997) shows significant differences on shallow V_p and V_s profiles of the sediments from in-situ measurements at Shelby Forest, TN; Marked Tree, AR; and Risco, MO. In their modeling of surface wave dispersion using V_p , V_s and thickness information of the sediments from adjacent well-logs, Dorman and Smalley (1994) concluded that the sediments in the embayment serve as an excellent wave-guide to excite very efficient surface waves from earthquakes inside the embayment than that from outside. Based on the relationship between the basin resonance and thickness of the basin fill, Bodin and Horton (1999) estimated average V_s of 834 m/sec and 960 m of thickness for the post-Paleozoic sediments beneath Memphis area.

Combining data from well-logs and from a few shallow seismic profiles, Mihills (1998) and Mihills and Van Arsdale (1999) subdivided the Post-Paleozoic sediments into layers based on lithology. Gao (1999) determines a representative 8-layer V_p and V_s model by summarizing all the available information assuming a constant V_p/V_s ratio inside each layer based on similar lithology. In the velocity model of Gao (1999), shallow V_p and V_s information are taken from a few shallow in-situ measurements (Liu et al., 1997) and from a few nearby shallow seismic reflection/refraction lines provided by UK (Figure 2). Deeper S-wave information is determined from a linear inversion of the arrival time differences between the direct S and the S-to-P converted waves. The 3-D V_p and V_s model for the sediments has been implemented into the initial model for a 3-D tomographic inversion to determine a 3-D crust model beneath the upper Mississippi Embayment (Gao, 1999) that has already had a significant impact in improving the hypocentral locations (Figure 4).



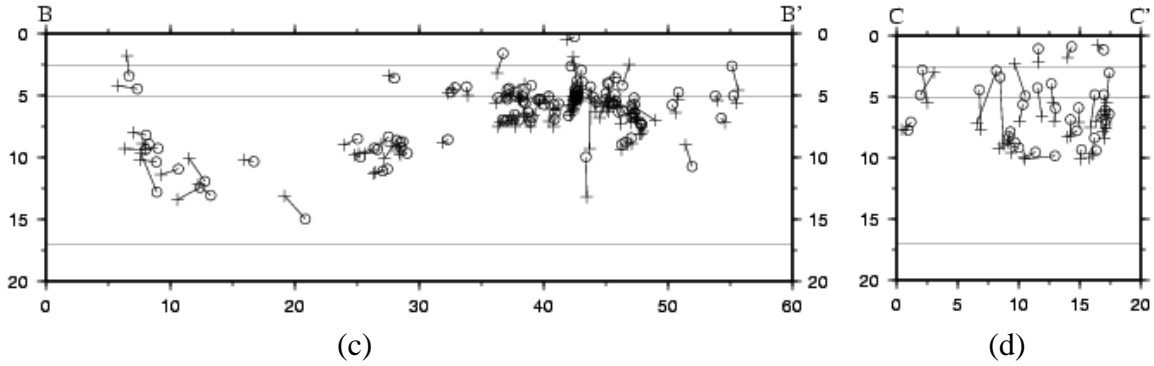


Figure 4. (a) Index map of three along-strike x-sections, hypocenters are relocated by applying a recently developed single-event location program using 3-D V_p and V_s models (Chen et al., 2006), (b) an along strike x-sectional view of hypocenters for the NE segment of the NMSZ showing the original locations (cross) and the 3D relocated hypocenters (open circle). The relocated hypocenters are, in general, shifted toward deeper depth as expected. (c) the same as (b) for the central segment of the NMSZ showing that the original and relocated hypocenters are very close to each other, and (d) the same as (b) for the SW segment of the NMSZ showing that the relocated hypocenters are consistently shifted upward.

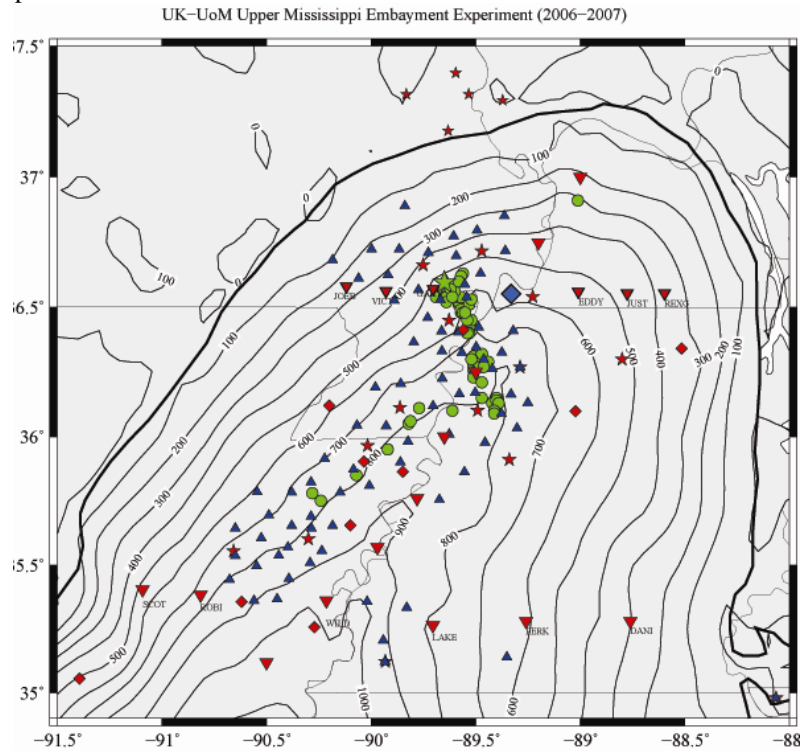


Figure 5. Map showing the locations of 20 selected sites (reverse red triangles) and UK's drilling site (blue diamond). Selected sites are along a northern EW line at $\sim 36.55^\circ\text{N}$, a southern EW line at $\sim 35.40^\circ\text{N}$, and an axial NE-SW line. Blue triangles and red stars are the CERI short-period and broadband seismic network stations, respectively. Green circles are the recent local earthquakes occurred in the NMSZ during the short deployment period of the broadband stations. Red diamonds are the locations of deep wells with logs.

Field Work and Data Analysis

Field Work Sites

A total of 20 sites are selected along three lines. Six sites are selected along an east-west northern line at 36.55°N across the drilling site of the University of Kentucky near Hickman, Kentucky. Another six sites are selected along an east-west southern line at 35.40°N slightly north of Memphis. Additional 8 sites are selected along the axial line of the Mississippi embayment.

These sites are selected to test if the entire column of post-Paleozoic sediments beneath sites of various sediment thicknesses can be explored by the new P and S source and also to test if velocity information between sites 20~30 km apart can be correlated. Most of our results presented in this report will focus on the northern and southern east-west lines.

Deployment of Portable Broadband Station

A portable broadband seismic station has been installed at each of the selected sites along the northern and southern east-west lines for a period of two to four weeks to record local, regional, and teleseismic earthquakes. Most sites along the axial line are located near CERI seismic network stations that no temporary seismic station has been installed. Earthquake data from the nearby CERI stations have been compiled to simulate for the converted wave study of the nearby site. Up to ten temporary broadband stations are deployed at one time. These temporary stations have been synchronized with GPS time and operated in continuous recording at 100 samples/sec. Site maintenance is needed once every two weeks to retrieve data and to replace battery.

Seismic Reflection/Refraction Lines

A seismic line using P- and S-wave sources has been conducted at each of the selected 20 sites. The UK group's newly acquired P- and S-wave source is a truck mounted device that uses a 3000 psi nitrogen spring to accelerate a 200 lbs slug into a steel anvil, creating a powerful ground-coupled impulse. It will generate P-wave source when the piston is oriented normal to the ground surface. The P-wave receivers are an inline spread of forty-eight 40-Hz vertical component geophones spaced at a 4 m interval. In order to overcome system saturation from the high energy seismic source, a 3lbs hammer is used at the array mid-point to investigate the very near-surface velocity (e.g., depth to water table). The P-wave source is stepped-out to offsets of one to four times the length of the geophone spread, as well as the zero offset, depending upon the length of the geophone spread, the quality of the recorded signal, and the depth to Paleozoic bedrock. The piston is rotated to approximately 45° with the ground surface to generate SH-wave. The source is also rotated to the opposing side in order to generate SH-waves with opposite polarity. The recording polarity of the seismogram is also reversed so that SH energy undergoes constructive interference and P-waves are suppressed. The mechanical field conversion from the P-wave to S-wave source is quick and efficient; consequently, both P- and S-wave seismic surveys can generally be accomplished in approximately 3 hours for any selected site (i.e. 2 to 3 sites per day). SH-wave data are also acquired at mid-point of the array using a hammer (3 lbs) striking an I-beam normal to the array as described in Street *et al.* (1995). Inline spreads of forty-eight 30-Hz (or 4.5 Hz) horizontally polarized geophones, spaced at 4 m interval are anticipated

Interpretation of Well Logs and Converted Waves

Sonic log data are available from 10 deep wells that penetrate into Paleozoic rocks beneath the sedimentary basin (Dart 1992). In addition, 35 deep wells (without logs) have also provided important constraints on the thickness of the sediments or depth to the top of Paleozoic rocks. Thickness of the sediments beneath each selected site can be estimated from an interpolation or extrapolation of information available from these 45 deep wells using the surrounding outcrops of the Paleozoic basement as references (Figure 1). Cross-sectional views of the bottom of the sedimentary basin along the ten E-W lines can be easily constructed from the contour lines (Figure 6). Well log information from these deep wells can provide very important constraints for a successful interpretation of Vp and Vs models from the seismic lines at the nearby sites.

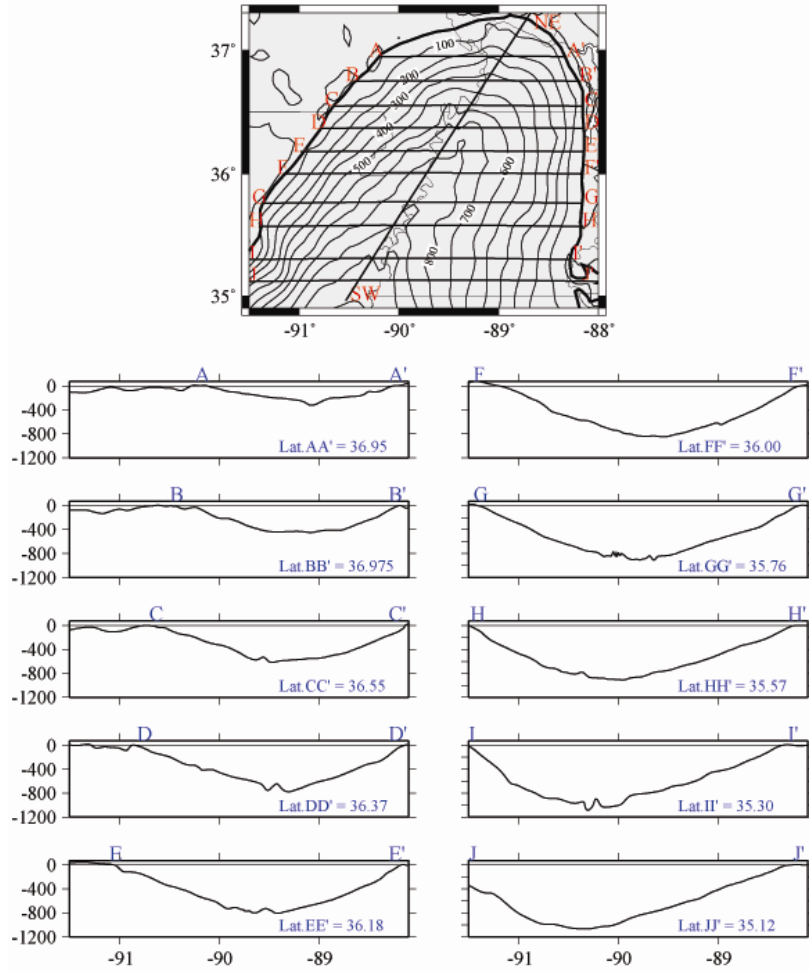


Figure 6. Index map (top) and ten Cross-sectional views of sedimentary basin along ten E-W lines (AA' to JJ') showing very significant lateral variation of thickness of sediments from north to south and from west to east. The contour lines and the bottom of the basin are determined from ~45 deep wells (Dart 1992, Gao 1999).

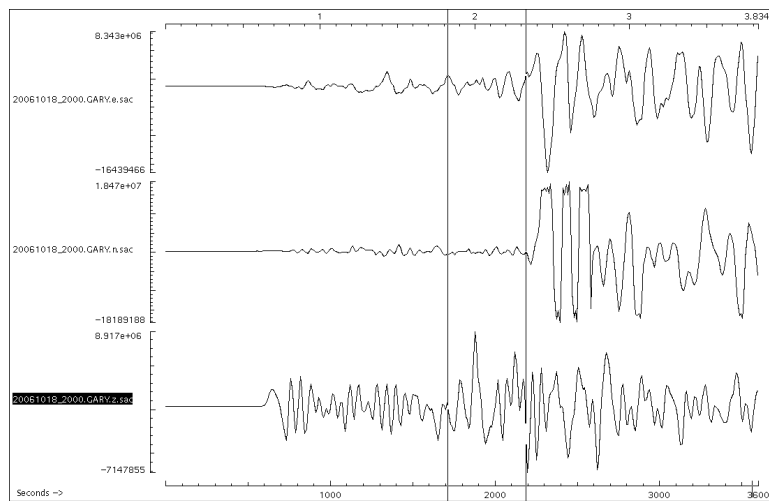


Figure 7. Direct S (1st vertical line from right) and converted Sp (2nd vertical line from right) arrivals identified from a typical 3-component (EW, NS, and Z from top down) seismogram recorded at a temporary BB station, GARY, near the town of New Madrid, Missouri.

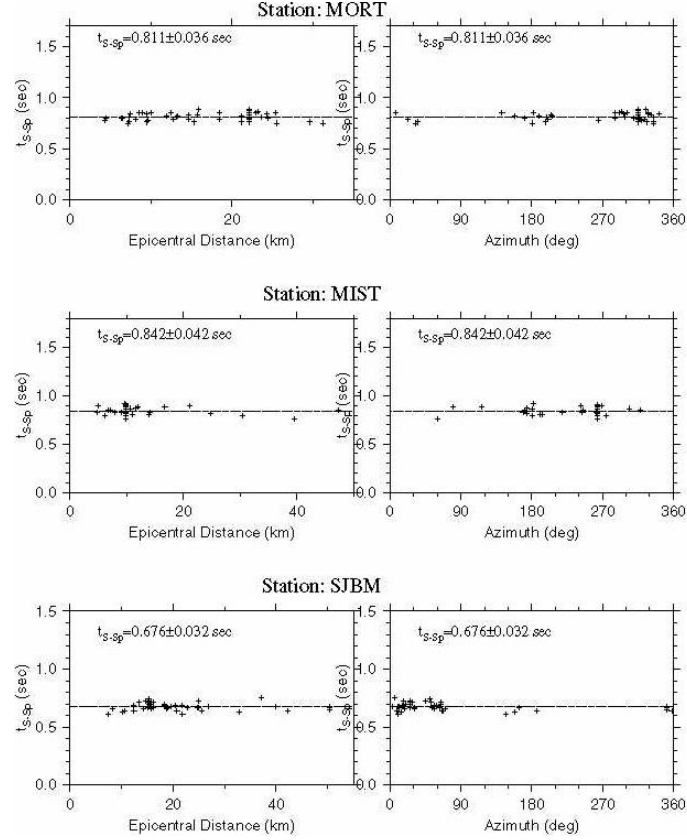


Figure 8. Plots of travel time difference (Δt_{S-S_p}) between the direct S and converted Sp waves versus epicentral distance (left) and azimuth (right) of earthquakes for three CERI stations showing that Δt_{S-S_p} is a constant for each station independent of the distances and azimuths of the earthquakes but are different between stations.

The impedance contrast between the Paleozoic basement rock ($V_p \approx 5.9$ km/s) and the overlying sediments ($V_p \approx 2.2$ km/s) is significant so that not only the incoming seismic waves will be amplified but also the non-vertical incident direct waves and the converted waves will propagate to the surface station almost vertically. Thus, the variations of arrival time differences (Δt_{S-S_p} and Δt_{P_s-P}) correspond to the difference in thickness and velocity distribution of the sediments beneath each station. We focus on the Sp phase because its arrival time is easier to pick on the vertical component than that for the Ps phase on the two horizontal components. As shown at three CERI stations (Figure 8), Δt_{S-S_p} for all earthquakes recorded at the same site are plotted against either epicenter distance, or azimuth, or depth of earthquakes. Therefore, a representative Δt_{S-S_p} for each selected site can be determined from a least-square fit of data similar to that shown in Figure 8. The representative Δt_{S-S_p} for each site can be used to validate the interpreted V_p and V_s models. Results from these studies will provide important constraints for the interpretation of V_p and V_s models from seismic lines and to verify the resultant V_p and V_s profile beneath each site.

Analysis and Interpretation of P- and S-wave Seismic Lines

The P - and SH -wave field files are processed on PCs using the commercial software package VISTA 7.0 (Seismic Image Software Ltd., 1996). Typical signal processing consists of

converting the raw files into SEG-Y format files, bandpass filtering, applying an automatic gain control (AGC), and using a frequency-wave number (FK) filter to remove residual ground roll. Timing corrections due to changes in elevation between the shotpoint and geophones will be included at sites with significant relief. The two-way intercept times and stacking velocities from interpreted P - and SH -waves reflections will be estimated using an interactive hyperbolic curve-fitting computer algorithm for the X^2-T^2 analysis. Interval velocities are then calculated using the Dix equation. First-break arrival times for the refracted SH -waves are interpreted by the seismic-refraction software package SIPT2 v.4.1 (Rimrock Geophysics, Inc., 1995) to derive S -wave velocity-depth model. SIPT2 uses the delay-time method to obtain a first approximation of the velocity-depth model by comparing the observed first-break picks to those computed using ray-tracing. The model is then iteratively adjusted to decrease the travel-time differences between the first-break picks and the model-calculated arrival times.

Inversion of the Deeper S-wave Velocity Information

Since S -wave generated by the new shear-wave source is not capable of sampling sediments deeper than 300 meters due to the limitation of the coupling of the plate to the ground, deeper V_s information for the deeper sediments can be determined following a linear inversion technique of Gao (1999). With the known thickness of sediments, V_p model, and V_s model for the upper 300 m, the V_s model for the deeper sediments can be inverted using a simple linear inversion of travel time differences Δt_{S-S_p} as *a priori* information. The generic equation of the inversion can be written as:

$$r = AY \quad (1)$$

Where $r = (\Delta t_{i0} - \Delta t_{ic})$, Δt_{i0} represents the observed time difference between the converted S_p wave and the direct S at the i th station. Δt_{ic} is the calculated time difference between S_p and S arrivals at the i th station. Here $i=1,2,3,\dots,n$, and n is the number of stations.

$$A = \begin{pmatrix} \left[\frac{\partial(\Delta t)}{\partial k_1} \right]_1 & \dots & \left[\frac{\partial(\Delta t)}{\partial k_m} \right]_1 \\ \vdots & \vdots & \vdots \\ \left[\frac{\partial(\Delta t)}{\partial k_1} \right]_n & \dots & \left[\frac{\partial(\Delta t)}{\partial k_m} \right]_n \end{pmatrix} \quad (2)$$

$$Y = \begin{pmatrix} \Delta k_1 \\ \vdots \\ \Delta k_m \end{pmatrix} \quad (3)$$

Where k_1, k_2, \dots, k_m are the V_p/V_s ratios in the $1^{st}, 2^{nd}, \dots, m^{th}$ velocity layers, respectively. $\Delta k_1, \Delta k_2, \dots, \Delta k_m$ are the corrections in the ratios to be determined in each iteration. The V_p/V_s ratio is assumed to be a constant inside each layer of similar lithology, although lateral variations of P - and S -wave velocities inside a layer may exist.

Because there are more observations than model parameters, the inversion process defined above (equation 1) is an over-determined system. The convergence of the inversion processes depends on the accuracy of the P -wave velocity model, how well the system is mathematically defined, and the initial model. The proposed method of linear inversion has been developed and

tested by Gao (1999) for the central NMSZ using a constant Vp and Vs values for the upper most two sedimentary layers for all stations. Therefore the Vs solution from this linear inversion is subjecting to a problem of non-uniqueness. This inversion process is still undergoing testing to calibrate the inversion resolution at sites where sediment thickness is less than 300 meters and complete Vp and Vs models are determined from seismic profile.

3-D Vp and Vs Models for the Post-Paleozoic Sediments and Their Applications

The 20 sites sample only very small portion of the embayment. Results from these 20 sites are not sufficient spatially to depict the complicated subsurface structure in the region. If there are sufficient sites in the future, the final product of the ongoing and future research will be a high-resolution 3-D Vp and Vs models for the post-Paleozoic sediments in the northern upper Mississippi Embayment by interpolating velocity models between the adjacent sites and using the outer boundary of the embayment as a reference. The observed arrival time difference between the direct S and converted Sp waves will then be used to verify the Vp and Vs profiles of sediments beneath each selected site. The resultant 3-D velocity model for the sediments can be used for the following applications that will constitute the research focuses of future NSF and/or NEHRP proposals:

- (a) calculate the expected strong ground shaking from future moderate to large earthquake in the NMSZ and to contrast the differences with other model.
- (b) construct a map of site-specific amplification factors from the largest impedance contrast in the sediments beneath each site and compare with the map from the Vs30 and soil classification.
- (c) determine 3-D crust and upper mantle Vp and Vs models from a 3-D tomographic analysis of P and S travel time data by including 3-D Vp and Vs models for the sediments in the initial models.
- (d) relocate all NMSZ events using 3-D crust Vp and Vs models and investigate 3-D geometry and properties of the active fault zones in the NMSZ.
- (e) model seismic response of 3-D basin from incoming seismic waves using finite-difference or finite-element modeling technique.

Preliminary Results

Preliminary results from this NEHRP project from March 2006 to Sept. 2007 are briefly reported here. P- and S-wave seismic reflection/refraction lines were completed at most of the selected 20 sites along the northern and southern east-west lines, a few sites along the axial line, and at UK's drilling site (Figure 5). Temporary broadband stations have been deployed at 13 of the 20 selected sites for a period of a few weeks to a couple months. Preliminary results from the ongoing project are briefly discussed below.

Preliminary Results from Seismic Lines

The UK's hydraulic-lift nitrogen-spring impact seismic source was damaged in early 2007 during field work near Jackson, TN after the completion of all sites in the northern line and the eastern most site of the southern line. Seismic lines at the reminding sites along the southern line and at a few sites along the axial line were completed in the fall and late 2007 after the seismic source was rebuilt. Summary results from seismic lines at most of 20 sites are reported here.

The seismic source is truck mounted for easy movement along the survey line. A 200 lbs piston is accelerated by a 3000 psi gas spring to generate P- and S-waves to sample sedimentary interfaces to 1000 m and 300 m, respectively. The penetration depth of the S-wave is limited by the coupling condition of the steel plate with the ground. Therefore, the seismic source will

generate P-waves to sample the entire sediment column and S-wave to sample the uppermost 300 m of sediments, e.g. along the southern EW line shown in Figure 5. Most importantly, it is very easy to convert from P-wave generator to SH-wave generator within a couple of minutes to facilitate a smooth progress in field environment. Typically, data from two to three sites can be collected in a single day assuming the sites have already been selected.

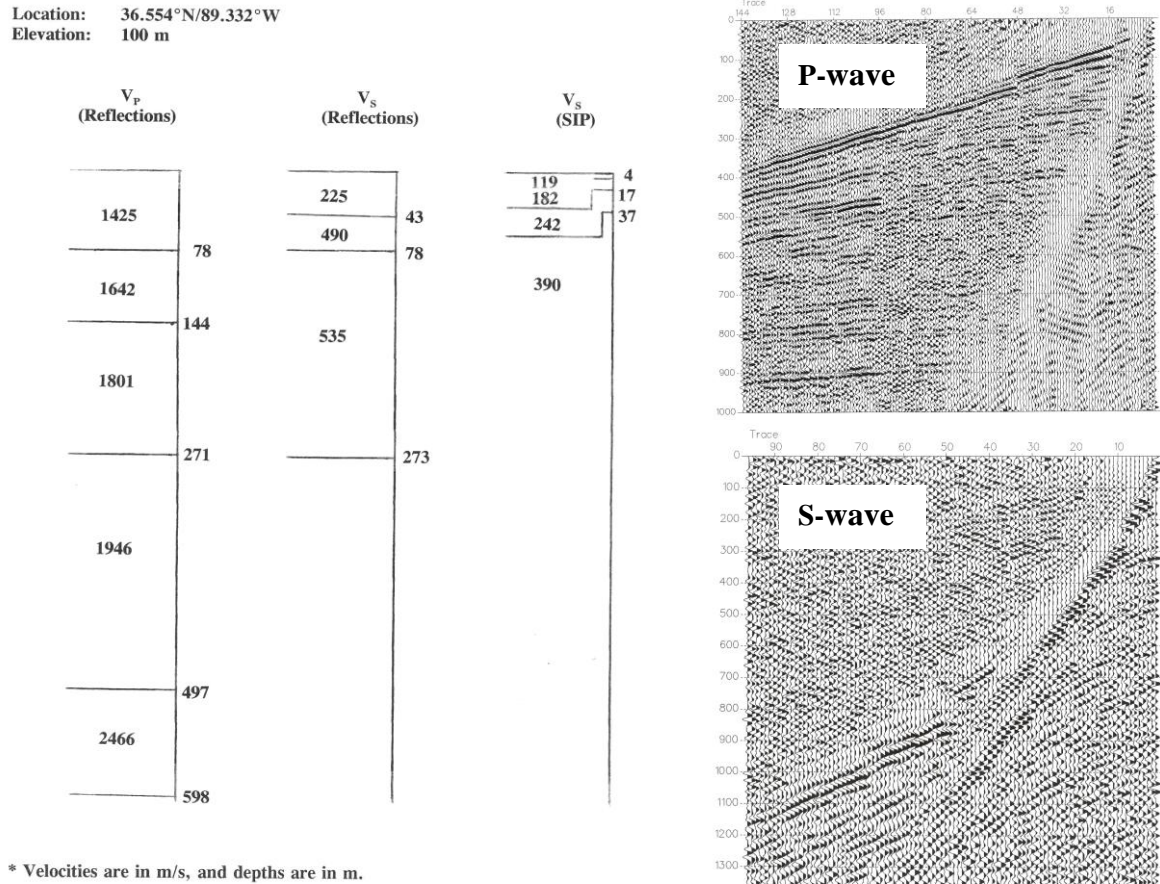


Figure 9. (Left) P- and S-wave velocity/depth models (depth shown along the side of column; no elevation correction) for the unlithified sediment near the UK's drilling site. (Right) Example of reflection/refraction seismograms obtained from shot gathers used to derive the V_p and V_s models. Trace space is 4 m.

Examples of P- and S-wave seismograms collected at the UK's drilling site and the interpreted V_p and V_s models are shown in Figure 9. In this example, V_p model for the entire thickness of sediments has been resolved but only the top 273 m of V_s model. P-wave energy can be efficiently coupled to ground plate to transmit P-wave to explore structures at deeper depth but apparently it is not the case for the SH wave source. We are currently in the processing of extending the SH model to deeper depth using a linear inversion technique developed by Gao (1999) to resolve V_s model for the deeper sediments with known thickness of sediments, known V_p for the entire sediments, known V_s of the upper part of the sediments, and the time difference between the direct and converted waves. Results of V_s model will be reported in the future. Nevertheless, significant lateral and vertical variations of V_p and V_s can be easily recognized from the examples shown here (Figure 10).

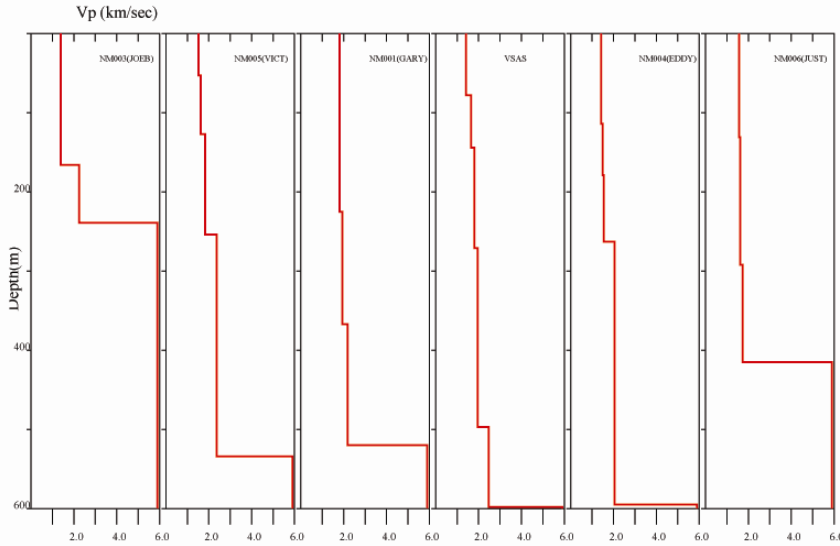
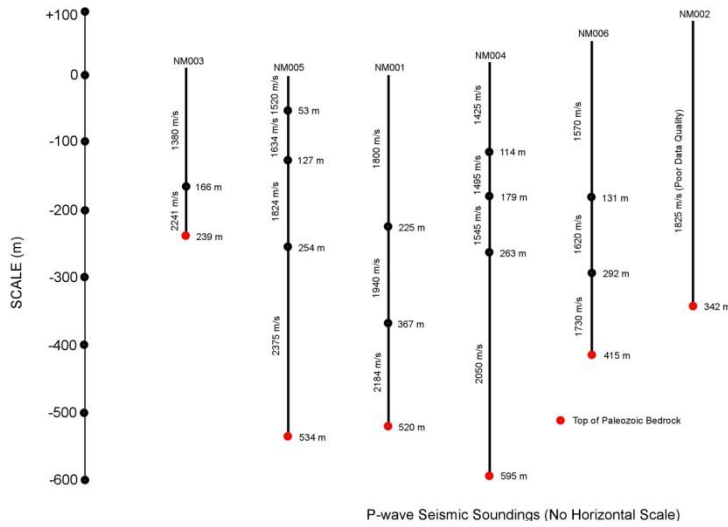


Figure 11a. An EW cross-sectional view of sediment profile showing the locations of the six selected sites (reverse green triangles), the CERI seismic station sites (reverse pink triangles), and the UK's drilling site (orange diamond). Top of the Paleozoic basement from the contour lines is marked by the blue line. Bottom of the sediments estimated from well logs and from the converted wave study is marked by solid blue and yellow circles, respectively.

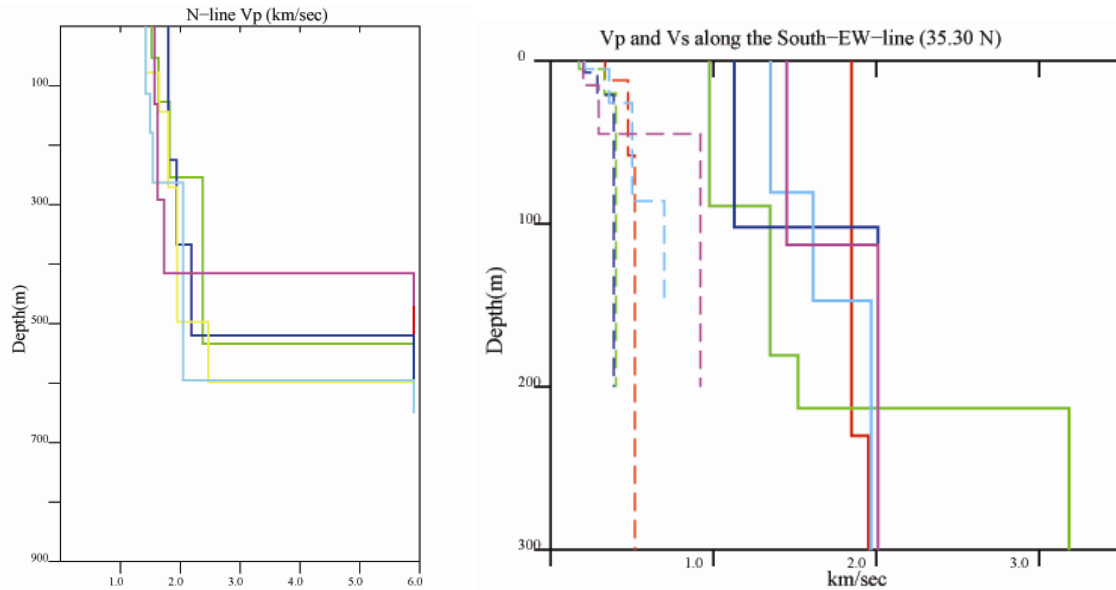


Figure 11b. Left: examples of Vp profiles at six sites along the northern EW line showing a Paleozoic basement at various depths with $V_p=5.9$ km/sec. Right: examples of shallow (shallower than 300 m) Vp (solid lines) and Vs (dash lines) profiles at five sites along the southern EW line. Very significant lateral and depth variations of Vp and Vs in the Post Paleozoic sediments are apparent that cannot be properly represented by any 1-D layered model. .

Examples of Vp and Vs profiles determined from seismic lines for the selected sites along the northern and southern lines are shown in Figure 11. It is consistent that the Paleozoic bedrock is characterized by a Vp of 5.9 km/sec at various depths beneath different sites. Significant lateral and vertical variations of Vp and Vs, especially in the upper most 200 meters, are apparent from these examples. Vp/Vs ratio for the uppermost sediments in some sites are larger than 11.0.

Preliminary Results from Earthquakes and Deep Wells

Using the outcrops of the Paleozoic basement around the embayment as references, contours of the bottom of the sediments can be constructed (Figure 1) from an extensive interpolation or extrapolation of the thickness information from ~45 deep wells (Dart 1992, Gao 1999). Thickness of the sediments at each of the selected sites can be estimated from these contour lines. Figure 8 shows one cross-section view of sediment sections along one E-W line at 36.55° N. UK's deep borehole reaches to the top of the Paleozoic basement at a depth of 585 m, consistent with the estimated 582 m from the contour data.

The arrival times of Sp (S converted to P at the bottom of the sediment) and direct S can be reliably identified from typical 3-component broadband seismograms (Figure 9). Assuming an average $V_p=1.8$ km/sec and $V_s=0.6$ km/sec for the sediments, thickness of the sediments can be roughly estimated from the arrival time differences (T_s-s_p) between the direct S and the converted Sp waves at each site (Figure 7). The estimated thickness of sediments beneath the sites along the C-C' shows that larger disagreement is apparent beneath the sites of thicker sediments and excellent agreement can be found beneath the sites of thinner sediments (Figure 11a).

The disagreement between the thickness of sediments from well log data and from the converted waves reveal that the assumption of constant $V_p=1.8$ km/sec and $V_s=0.6$ km/sec is inadequate, especially for the region of thicker sediments. This result also confirms the report of Chen et al., (1996) that the average Vs is higher beneath the thicker sediments than that beneath the thinner sediments. When the Vp and Vs models are determined from the seismic reflection/refraction lines, the calculated thickness of sediments from the converted waves is expected to agree well with that from the well logs or the contour lines. The agreement of

thickness of sediments calculated from converted waves using the V_p and V_s models obtained from the seismic lines and obtained from well logs validates the reliability of the resultant V_p and V_s models. Thus, the well-log data, converted wave analysis, and the V_p and V_s models from seismic lines provide us mutually inclusive information to improve our understanding of the sediments in the embayment.

Anomalous P-wave Precursor

During the field deployment of portable broadband stations, anomalous P-wave precursor ~4 sec before impulsive P arrival (Figure 12) has been observed at station ~56 km from an epicenter at 10km depth beneath the New Madrid, Missouri. This distance is too short for a P_n wave. Unfortunately, we are not able to figure out apparent velocity of this precursor at this time due to not enough stations in that area and not enough time period of recording. But definitely, this is one of the research topics to be explored in the future seismological research in the area.

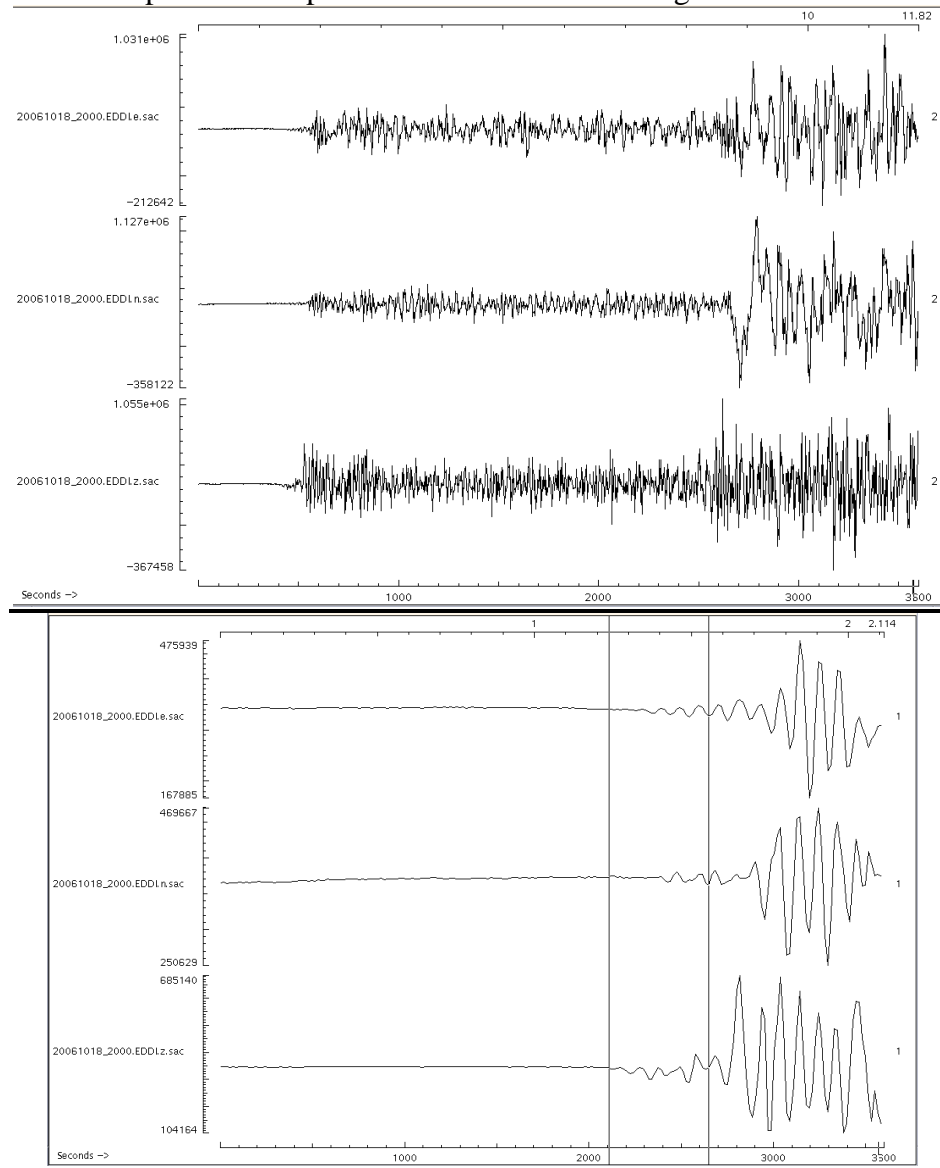


Figure 12. Typical 3-component broadband seismogram from a shallow earthquake (depth=10 km) near New Madrid, Missouri showing a small amplitude precursor ~4 seconds before the impulsive P-wave arrival. It will be a research topics in the future to explore whether this is a site specific feature or a reflection phase from deeper crustal interfaces.

Summary

The preliminary results from this project clearly demonstrate that high-resolution Vp and Vs structural model for the unconsolidated sediments can be determined at any selected site in the upper Mississippi Embayment by combining seismic lines and earthquake data. Site specific impedance profiles are different even between the adjacent sites. We also demonstrate that lateral and depth variations of Vp and Vs structures in the embayment are significant. Therefore a realistic estimation of site-specific amplification factor and a better modeling of strong ground motions in the embayment cannot rely on a simple Vs30 or 1-D model. Damage patterns from the 1985 Mexico City, 1988 Armenia, 1989 Loma Prieta, 1994 Northridge, 1999 Chi-Chi, and 2001 Gujarat earthquakes reveal that the nature, severity, and duration of strong ground shaking depend significantly on the size and location of potential earthquake source, geometry and mode of movement along active faults, 3-D basin response, site-specific soil conditions and its seismic response, and other geotechnical factors. From studies of damage patterns (e.g. Bard and Bouchon 1985, Frankel and Vidale 1992, Paolucci et al. 1992, Frankel 1993, Graves 1993), serious questions have been raised about the validity of strong ground motion predictions based on a simple 1-D simulation. For example, Frankel (1993) noted that synthetic seismograms obtained from 2-D and 3-D modeling of basins exhibited large surface waves produced by the conversion of S-waves at the edge of the basin. Boore (1999) noticed that the response spectra of strong ground motions in the Los Angeles basin might be as much as 5 to 10 times larger than expected from standard response spectra predictions for the basin based on 1-D simulations. Thus, the integration of SH- and P-wave velocity measurements, drill hole depths, seismic sections, and sonic logs will provide us with well-constrained 3-D Vp and Vs models of the post-Paleozoic sediments throughout the upper Mississippi Embayment. Knowledge of the deeper sediments is critical to ground motion modeling (Anderson et al. 1996). Major impedance boundaries within the post-Paleozoic sediments, especially at shallow depth, in the upper Mississippi Embayment will also have a significant impact on the amplification and linearity/nonlinearity assessment of the strong ground motions throughout the region. Therefore, a realistic assessment of strong ground motion in the embayment is possible only when comprehensive 3-D Vp and Vs models for the sedimentary basin is available. From 3-D Vp and Vs models for the sediments, the method developed for earthquake hazard maps of the Memphis area (e.g. Gombert et al. 2003; Cramer et al., 2004) can then be applied to the entire upper Mississippi Embayment in a similar but slightly different approach as Cramer (2006).

Future Research Plan

Results from seismic profiles as briefly presented earlier (Figure 11) have shown adequate resolution of Vp and Vs profiles for the sediments that are correlated well with the information available from the adjacent deep wells. Validation also comes from the analysis of converted waves from the bottom of the sediments. In a pending NEHRP proposal, we plan to conduct similar experiment at 90 additional sites evenly distributed over the entire upper Mississippi Embayment (Figure 13). Integration of Vp and Vs structural information from ~110 sites, a representative 3-D Vp and Vs model for the entire upper Mississippi Embayment can be achieved. Modeling of 3-D basin response, realistic estimation of site specific amplification and strong ground motion, and other pertinent research targets important for a successful seismic hazard assessment can thus be accomplished.

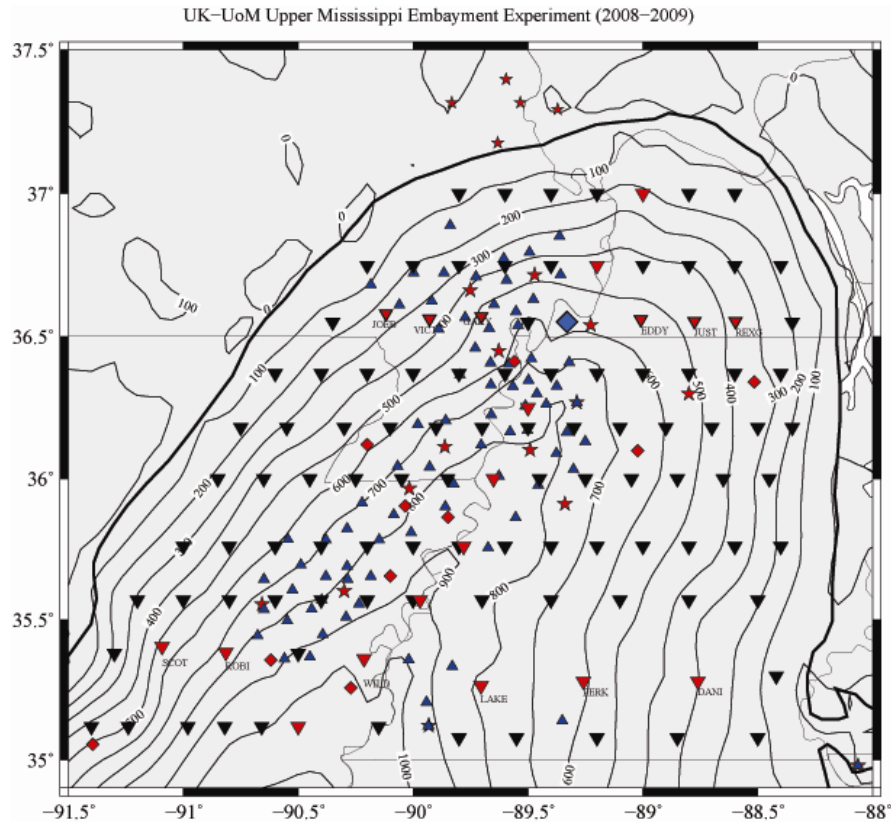


Figure 13. Planned additional 90 sites (reverse black triangles) in a pending NEHRP proposal and the 20 sites from the previous USGS project (reversed red triangles) along 10 E-W lines. Blue diamond is UK's deep drilling site where top of the Paleozoic basement is found at 585 m from the surface. This depth is consistent with the 582 m determined from the well log data. Red stars and blue triangles are the CERl BB and short-period seismic network stations, respectively. Red diamonds are the locations of deep boreholes with sonic and other logs.

Acknowledgement

We would like to express our sincere thanks to many friendly land owners in Kentucky, Missouri, Arkansas, and Tennessee who kindly allow us to deploy portable seismic stations and conduct seismic survey in their properties. They include Charles Eddie Williams, Joe Bader, Gary Carl, Rex Gilbert, Victor Rhonda Roth, Justus Willet, Steve Perkins, Robert McPherson, Danny Hopper, Scott David Hanley, Glen R. Miller, and a few more.

References

- Anderson, J.G., Y. Lee, Y. Zeng, and S. Day, (1996). Control of strong motion by the upper 30 meters. *BSSA*. 86, 1749-1759.
- Andrews, M.C., W.D. Mooney, and R.P. Meyer, (1985). The relocation of microseismicity in the northern Mississippi embayment, *JGR*. 90, 10223-10236.
- Bard, P.-Y. and M. Bouchon, (1985). The seismic response of sediment-filled valleys. Part II. The case of incident P and SV waves. *BSSA*. 70, 1921-1941.
- Bauer, R.A., (2004), Final technical report: central U.S. shear wave velocity database with accompanying geological/geotechnical information of nonlithified geologic materials external grand award number 04-HQ-GR-0074, CUSEC State Geologists, p 29.

- Bodin, P. and S. Horton, (1999). Broadband microtremor observation of basin resonance in the Mississippi embayment, Central U.S. *GRL*, 26, 903-906.
- Boore, D.M., (1999). Basin waves on a seafloor recording of the 1990 Upland, California, earthquake; Implications for ground motions from a larger earthquake. *BSSA*. 89, 317-324.
- Carver, D. and S.H. Hartzell, (1996). Earthquake site response in Santa Cruz, California. *BSSA*. 86, 55-65.
- Chen, H., J.M. Chiu, J. Pujol, K.H. Kim, K.C. Chen, B.S. Huang, Y.H. Yeh, and S.C. Chiu, (2006), A simple algorithm for local earthquake location using 3-dimensional Vp and Vs models – test examples in the central USA and Taiwan regions, *Bull. Seismo. Soc. Am.*, 96(1), 288-305.
- Chen, K.C., J.M. Chiu, and Y.T. Yang, (1994). Q_p - Q_s relation in the sedimentary basin of the upper Mississippi embayment using converted phases, *BSSA*. 84, 1861-1868..
- Chen, K.C., J.M. Chiu, and Y.T. Yang, (1996). Shear-wave velocity of the sedimentary basin in the Upper Mississippi embayment using S-to-P converted waves, *BSSA*. 86, 848-856.
- Chen, K.C., (2003). Strong ground motions and damages in Taipei Basin from the Moho reflected seismic waves during the March 31, 2002, Hualien, Taiwan earthquake, *GRL*, 30(11), doi:10.1029/2003GL017193.
- Chiu, J.M., A.C. Johnston and Y.T. Yang, (1992). Imaging the active faults of the central New Madrid seismic zone using PANDA array data. *Seismo. Res. Lett.*, 63, 375-393.
- Cramer, C.H., (2001). Preliminary site amplification investigation for the Memphis-Shelby county area of Tennessee using Vs30, *Seismo. Res. Lett.*, 72(1), 127.
- Cramer, C.H., J.S. Gomberg, E.S. Schweig, B.A. Waldron, and K. Tucker, (2004). The Memphis, Shelby County, Tennessee, Seismic Hazard Maps, *U.S. Geol. Surv. Open-File Report* 04-1294.
- Cramer, C.H., (2006), Quantifyinf the uncertainty in site amplification modeling and its effects on site-specific seismic hazard estimation in the upper Mississippi Embayment and adjacent areas, *BSSA*, 96(6), 2008-2020.
- Dart, R.L., (1992). Catalog of pre-Cretaceous geologic drill-hole data from the UpperMississippi Embayment: A revision and update of Open-File Report 90-260, *USGS, Open-File Report*, 92-685, 253 pp.
- Dorman, J., and R. Smalley, (1994). Low-frequency seismic surface waves in the Upper Mississippi Embayment, *SRL*, 65, 137-148.
- Frankel, A., (1993). Three-dimensional simulations of ground motions in the San Bernardino Valley, California, for hypothetical earthquakes from a Loma Prieta aftershock, *BSSA*. 82, 2045-2074.
- Frankel, A. and J. Vidale, (1992). A three-dimensional simulation of seismic waves in the Santa Clara Valley, California, from a Loma Prieta aftershock. *BSSA*., 83, 2045-2074.
- Frankel, A., D. Carver, E. Cranswick, T. Bice, R. Sell, and S. Hanson, (2001). Observations of basin ground motions from a dense seismic array in San Jose, California, *BSSA*, 91(1), 1-12.
- Gao, F.C., (1999). High-resolution 3-D sedimentary basin and upper crustal structures from 3-D inversion of PANADA data, M.S. thesis, The University of Memphis.
- Gomberg, et al. (2003). Lithology and shear-wave velocity in Memphis, Tennessee, *BSSA*, 93(3), 986-997.
- Graves, R.W., (1993). Modeling three-dimensional site response effects in the Marina District Basin, San Francisco, California. *BSSA*. 83, 1242-1263.
- Hwang, H., S. Pezeshk, W.W. Lin, J. He, and J.M. Chiu, (2001). Generation of synthetic ground motion, Mid-America Center, CD Release 01-02.
- Johnston, A.C., (1982). A major earthquake zone on the Mississippi. *Scientific. Amer.*, 246, 60-68.
- Kim, K.H., J.M. Chiu, J. Pujol, K.C. Chen, B.S. Huang, and Y.H. Yeh, (2005). Three-dimensional Vp and Vs structural models associated with the active subduction and collision tectonics in the Taiwan region, *Geophys. J. Int.*, **162**, 204-220.
- Liu, H.P., Y. Hu, J. Dorman, T.S. Chang, and J.M. Chiu, (1997). Upper Mississippi Embayment shallow seismic velocities measured in situ, *Engineering Geology*, 46, 313-330.
- Mihills, R.K., (1998). A structural anlaysis of the New Madrid seismic zone from contour maps and a three-dimensional model, M.S. Thesis, The University of Memphis.

- Mihills, R.K., and R.B. VanArsdale, (1999). Late Wisconsin to Holocene New Madrid seismic zone deformation, *BSSA*, 89, 1019-1024.
- Mooney, W.D., M.C. Andrews, A. Ginsberg, D.A. Peters, and R.M. Hamilton, (1983). Crustal structure of the northern Mississippi embayment and a comparison with other continental rift zones, *Tectonophysics*, 94, 327-348.
- Paolucci, R., M.M. Suarez, and F.J. Sanchez-Sesma, (1992). Fast computation of SH seismic response for a class of alluvial valleys. *BSSA*, 82, 2075-2086.
- Pujol, J. A. Johnston, J.M. Chiu, and Y.T. Yang, (1997). Refinement of thrust faulting models for the central New Madrid seismic zone, *Engineering Geology*, 46, 281-298.
- Rimrock Geophysics, Inc., (1995). SIPT2 V-4.1 (and other programs), 56 p.
- Seismic Image Software Ltd., (1996). VISTA 7.0 Notes, 477 pp.
- Street, R., E. Woolery, Z. Wang, and J. Harris (1995). A short note on shear-wave velocities and other site conditions at selected strong-motion stations in the New Madrid seismic zone. *SRL*, 66(1), 56-63.
- Street, R., E. Woolery, Z. Wang, and I.E. Harik, (1997a). Soil classifications for estimating site-dependent response spectra and seismic coefficients for building code provisions in western Kentucky. *Engineering Geology* 46, 331-347.
- Street, R., Z. Wang, E. Woolery, J. Hunt, and J. Harris, (1997b). Site effects at a vertical accelerometer array near Paducah, Kentucky. *Engineering Geology* 46, 349-367.
- Street, R., E. Woolery, Z. Wang, and J. Harris, (2001). NEHRP soil classifications for estimating site-dependent seismic coefficients in the central Mississippi River Valley. *Engineering Geology* 62, 123-135.
- Wen, K.L., L.Y. Fei, H.Y. Peng, and C.C. Liu, (1995), Site effect analysis from the records of the Wuku downhole array, *TAO*, v. 6, no. 2, 285-298.
- Williams, R.A., S. Wood, W.J. Stephenson, J.K. Odum, M.E. Meremonte, and R. Street, (2003). Surface seismic-refraction/reflection measurement determinations of potential site resonances and the areal uniformity of NEHRP site class D in Memphis, Tennessee: *Earthquake Spectra*, v. 19, 159-189.
- Williams, R.A., W.J. Stephenson, A.D. Frankel, and J. Odum, (1997). Surface seismic measurements of near-surface P- and S-wave seismic velocities at earthquake recording stations, Seattle, Washington, *Earthquake Spectra*, 15(3), 20p.
- Williams, R.A., W.J. Stephenson, A.D. Frankel, and J.K. Odum, (2001). Using high-resolution surface seismic imaging to study earthquake site response, 2001 GSA annual meeting.
- Wills, C.J., and W. Silva, (1998). Shear-wave velocity characteristics of geologic units in California, *Earthquake Spectra*, 14(3), 533-556.
- Woolery, E., R. Street, Z. Wang, and J. Harris, (1993). Near-surface deformation in the NMSZ seismic zone as imaged by high resolution SH-wave seismic methods. *SRL*, 64, 187-200.
- Woolery, E., R. Street, Z. Wang, and J. Harris, (1996). A P- and SH-wave seismic reflection investigation of the Kentucky Bend Fault Scarp in the NMSZ, *SRL*, 67, 67-74.
- Woolery, E., R. Street, Z. Wang, J. Harris, and J. McIntyre, (1999). Neotectonic structures in the central NMSZ: evidence from multimode seismic reflection data. *SR.*, 70, 554-576.
- Woolery, E. and R. Street, (2001). 3D near-surface soil response of earthquake engineering interest from H/V ambient noise ratios. Expanded Abstract, *10th International Conference on Soil Dynamics and Earthquake Engineering*, Philadelphia, Penn., Oct. 7-10.
- Woolery, E., and R. Street, (2002). Near-surface soils response from H/V ambient noise ratios, *Journal of Soil Dynamics and Earthquake Engineering*, v. 22, p. 865-876.
- Yang, Y.T., (1992). Fault zone geometry and crustal velocity structures in the central New Madrid seismic zone using data from the PANDA seismic array, M.S. thesis, The University of Memphis, 72 pp.